JOINT EUROPEAN TORUS

JET–P(90)43

J.O'Rourke and JET Team

The Change in the Safety Factor Profile at a Sawtooth Collapse

The Change in the Safety Factor Profile at a Sawtooth Collapse

J.O'Rourke and JET Team*

JET-Joint Undertaking, Culham Science Centre, OX14 3DB, Abingdon, UK

** See Appendix 1*

Preprint of Paper to be submitted for publication in
Plasma Physics and Controlled Fusion

ABSTRACT.

Perturbations of the electron density and the poloidal magnetic field induced by sawtooth instabilities are studied using interferometric and polarimetric data. The change in the safety factor profile at a sawtooth collapse is deduced. It is found that sawteeth do not lead to complete reconnection of the poloidal flux since $(\Delta q_o)^{collapse} < 1 - q_o$. A comparison of the rate of change of qo between sawteeth with field diffusion calculations assuming neo-classical resistivity also suggests that complete reconnection does not take place.

INTRODUCTION

The behaviour of the safety factor profile in sawtoothing plasmas has been the object of numerous experimental [1 – 8] and theoretical (eg. [9,10]) investigations. Several experiments [6 – 8] have reported values of the axial safety factor, q_o, close to 1, but others [1 – 5], including JET, have measured q_o to be below 1, outside of experimental errors. The latter results suggest that complete reconnection of the poloidal flux does not necessarily take place at a sawtooth collapse. The mechanism which would halt the reconnection process once it has begun is not understood.

In this context, one ambiguity associated with many of the measurements stems from their lack of temporal resolution, so that the quoted values of q_o represent an average over a sawtooth period [3,4,6,7]. A value of q_o below 1 can then arise if q_o remains below 1 throughout the sawtooth period (incomplete reconnection) but it can also arise if q_o is initially 1 after the sawtooth collapse (complete reconnection) but descends to a value less than the measured value--perhaps through an anomalously rapid diffusion of the current profile--before the next sawtooth collapse.

The aim of this paper is to quantify, through properly time- resolved measurements, the change in the axial safety factor, Δq_o, (and hence the amount of reconnection) which takes place at a sawtooth. Since this quantity can be related through field diffusion calculations to the value of q_o which obtains immediately following a sawtooth, a further aim is to verify whether the measurements of Δq_o are consistent with measurements of the absolute value of q_o

METHOD

The data used in this study have been obtained using JET's 6-channel far-infrared (0.195 mm.) polari-interferometer [11]. This instrument has a Mach-Zehnder configuration (see Figure 1). A heterodyne detection system with a 100 KHz modulation frequency is used. Thus the line-integrated electron density, $\int n_e dl$, is measured with a time resolution of 10 μs. The Faraday angle, $\sim \int n_e B_{\|} dl$, is measured using a lock-in technique and has a time resolution of 1 - 10 ms, determined by the selectable integration time of the electronics. Because these times are short with respect to the sawtooth period ($> 100ms$), sawteeth are clearly discernible in the raw interferometric and polarimetric data, (see Fig. 2),

and it is not necessary to perform a coherent averaging over many sawteeth in order to extract the signals.

In order to obtain maximum sensitivity to changes in the data, use is made of the linearity of the Abel transform [12]. Thus the local change in a quantity is calculated from the Abel-inversion of the change in the corresponding line-integrals.

Following [13], the change in the Faraday angle at a sawtooth, $\Delta\alpha$, is written as a first order expansion in the parallel magnetic field, $B_{\|}$, the electron density, n_e, and the integration path

$$\Delta\alpha = \Delta\left(C \int n_e B_{\|} dl \right) \simeq C \int (\Delta n_e) B_{\|} dl + C \int n_e (\Delta B_{\|}) dl + C (\Delta \int) n_e B_{\|} dl$$

where the last term takes into account the change in the Shafranov shift which occurs at the sawtooth collapse.

The change in the Faraday rotation angle due to the change in the poloidal field is obtained by subtracting from the total change the contributions from the perturbations of the density and the integration path. These "reduced" differential data are then Abel-inverted to obtain the change in the poloidal field in the same way that the total angles are used to derive the total poloidal field.

Figure 3 illustrates the steps in the analysis. Abel-inversion of the interferometric data yields the electron density profile (a). A smooth curve is passed through the Faraday rotation data (b). Use is also made of measurements of the poloidal magnetic field near the plasma boundary and of symmetry properties implied by the flux surface geometry by introducing "virtual" data points [11]. The poloidal magnetic field (c) is obtained by Abel-inversion of the Faraday angles using the electron density profile, and from this the safety factor profile (d) is calculated. The change in the electron density profile (e) is calculated by Abel-inversion of the change in $\int n_e\, dl$ at the sawtooth collapse. The contributions to the total change in the Faraday angles due to the change in the electron density and the Shafranov shift are subtracted to give the "net" contribution due to the change in the poloidal field (f). This is Abel-inverted to yield the local change in the poloidal field (g) and the corresponding change in the safety factor profile (h). An important source of error is the perturbed electron density, which gives rise to a change in the Faraday rotation angles that can be greater than the change

due to the perturbation in the poloidal magnetic field. It is estimated that the change in q_o can not be evaluated to better than $\pm$ 50%.

Note that the inferred change in the q-profile extends beyond the q = 1 surface. This is in qualitative agreement with observations of sawteeth in the presence of "Snakes" [14], which showed a radial contraction of the q = 1 surface during a sawtooth collapse.

In the example shown here $q_o = 0.7 \pm 0.2$ while $(\Delta q_o)^{collapse} = 0.03 \pm 0.02$. Hence these measurements imply that complete reconnection of the poloidal flux does not take place at a sawtooth collapse.

COMPARISON WITH FIELD DIFFUSION CALCULATIONS

In steady-state, the change in the q-profile at the sawtooth collapse is balanced by an equal and opposite change during the period between sawteeth. Thus the quantity $(\Delta q_o)^{collapse}/\tau_s$, where τ_s is the sawtooth period, is a measure of the rate of current diffusion between sawteeth. (The assumption of steady-state can be relaxed if the change in q_o during the sawtooth ramp rather than at the sawtooth collapse is considered.)

Figure 4 shows the behaviour $(\Delta q_o)^{collapse}$ as a function of τ_s for a number of 3 MA ohmic and ICRF heated JET discharges. The addition of ICRF power ($\leq$ 10 MW) lengthens the sawtooth period--leading ultimately to "Monster" sawteeth [15]--and allows a range of over one decade in τ_s to be studied.

With the assumption that the sawtooth instability leads to complete reconnection, the evolution of q_o may be modelled by solving the diffusion equation:

$$\frac{1}{r}\frac{\partial}{\partial r}\left(r\frac{\partial \eta j}{\partial r}\right) = \mu_o \frac{\partial j}{\partial t}$$

and introducing a periodic redistribution of the current density, j. This calculation has been performed for the discharges considered above. Cylindrical symmetry was assumed, and the Kadomtsev prescription for the reconnection process [9] was approximated by flattening the current density within the q = 1 surface. The resistivity, η was computed using a neo-classical expression, [16], and the measured electron temperature and effective charge. The calculated change in q_o during a sawtooth period

is shown as the upper band in Figure 4. The width of the band indicates the scatter in these diffusion calculations. The relatively weak dependence of this quantity on the sawtooth period results from the correlation between τ_s and the electron temperature in the data used here: for longer sawtooth periods the q-profile has more time to evolve, but the rate of diffusion is also slower.

For short sawtooth periods, the values of Δq_o calculated assuming complete reconnection are typically 2 to 5 times larger than the experimentally inferred values. This suggests that the actual q-profile following a sawtooth collapse is closer to the fully diffused state towards which it is evolving (given by a radially constant electric field) than complete reconnection would allow. Indeed, if sawtoothing is interrupted in the field diffusion calculation, q_o decreases rapidly at first and then increasingly slowly as the electric field becomes radially more uniform (Fig. 5). The lower band in Figure 4 shows the change in q_o during a time corresponding to a sawtooth period with q_o initially equal to 0.75. Note that for longer sawtooth periods, the rate of current diffusion is less dependent on the precise initial conditions and it is not surprising that the two bands begin to coalesce. However, for short sawtooth periods, the lower band lies within the error bars of the measurements, while the upper band does not. In this sense it may be concluded that these measurements of $(\Delta q_o)^{collapse}$ are consistent with the measurements of q_o itself, which indicate that it is below unity even immediately after a sawtooth collapse.

CONCLUSION

The perturbations to the q-profile induced by sawteeth have been studied using differential interferometric and Faraday rotation measurements. The magnitude of $(\Delta q_o)^{collapse}$ implies that complete reconnection does not occur in JET sawteeth both because it is much less than $1 - q_o$ and because the rate of current diffusion between sawteeth which may be deduced from it is inconsistent with an initial condition of $q_o = 1$ following the collapse.

REFERENCES

[1] H Soltwisch, et al.
Plasma Physics and Controlled Nuclear Fusion Research 1986
(IAEA, Vienna, 1987) Vol. I, p. 433

[2] J O'Rourke, et al.
Proc. 15th European Conference on Controlled Fusion and Plasma heating (EPS, Dubrovnik, 1988) Vol 12B (I), p. 155
J Blum, et al..
JET Report, JET-P(89)63. To be published in Nuclear Fusion.

[3] F M Levinton, et al.
Phys. Rev. Lett. 63(1989)2060

[4] W P West, et al.
Phys. Rev. Lett. 58(1987)2758

[5] M J Forrest, et al.
Nature 71(1978)718

[6] K McCormick, et al.
Phys. Rev. Lett. 58(1987)491

[7] D Wroblewski, et al.
Phys. Rev. Lett. 61(1988)1724

[8] H Weisen, et al.
Phys. Rev. Lett. 62(1989)434

[9] B B Kadomtsev
Fiz. Plazmy 1(1975)710

[10] J A Wesson
Plasma Physics and Controlled Fusion 28(1986)243

[11] G Braithwaite, et al.
Rev. Sci. Inst. 60(1989)2825

[12] R S Granetz and P Smeulders
Nuclear Fusion 28(1988)457

[13] H Soltwisch and W Stodiek
29th Ann. Mtg., APS Division of Plasma Phys, 1987
Paper 8V29

[14] A Weller, et al.
Phys. Rev. Lett. 59(1987)2303

[15] D J Campbell, et al.
Phys. Rev. Lett. 60(1988)2148

[16] Y B Kim, et al.
JET Report, JET-R(88)02

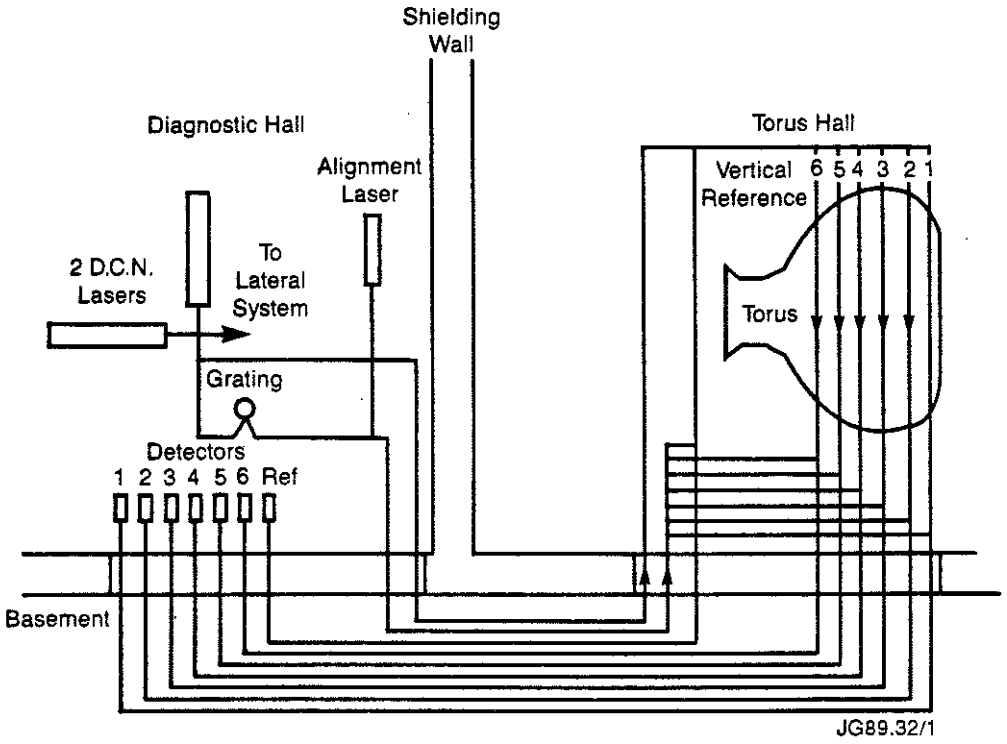

Fig. 1--Schematic of the vertical system of the JET interferometer.

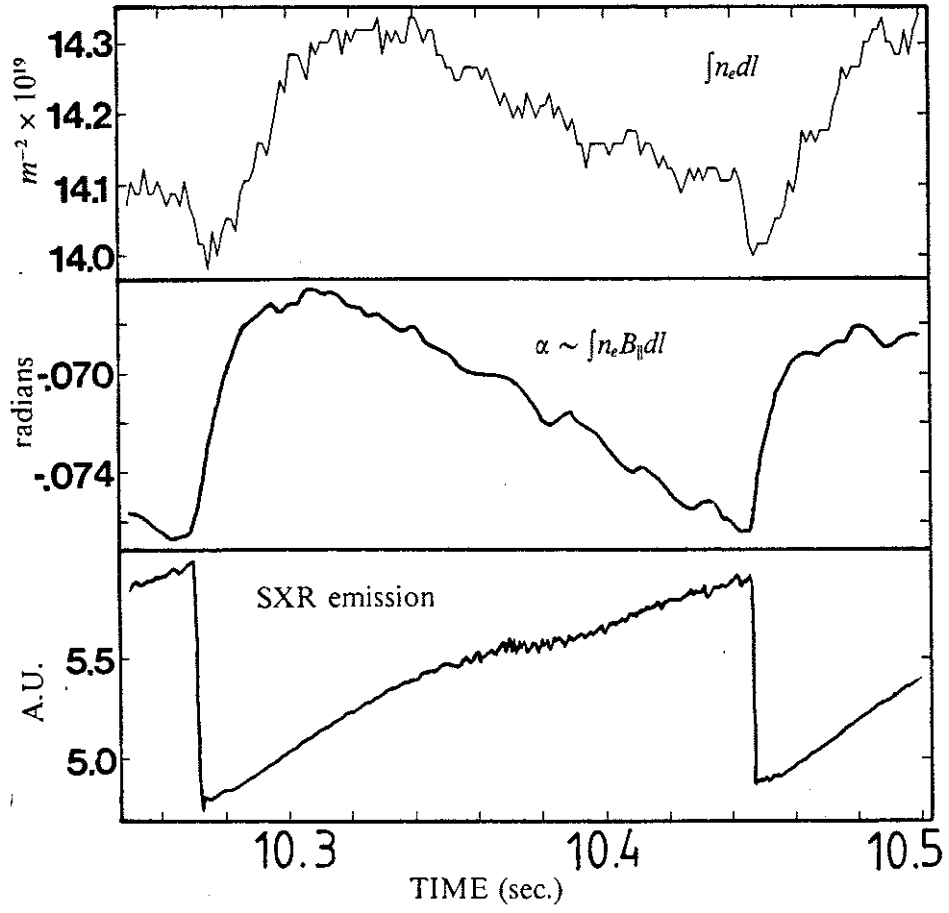

Fig. 2--Line-integrated electron density and Faraday rotation angle measured on a central chord (R = 3.02 m) during a sawtooth cycle. Also shown is a Soft X-ray signal. (Pulse #20639, 3MA, 2.2T).

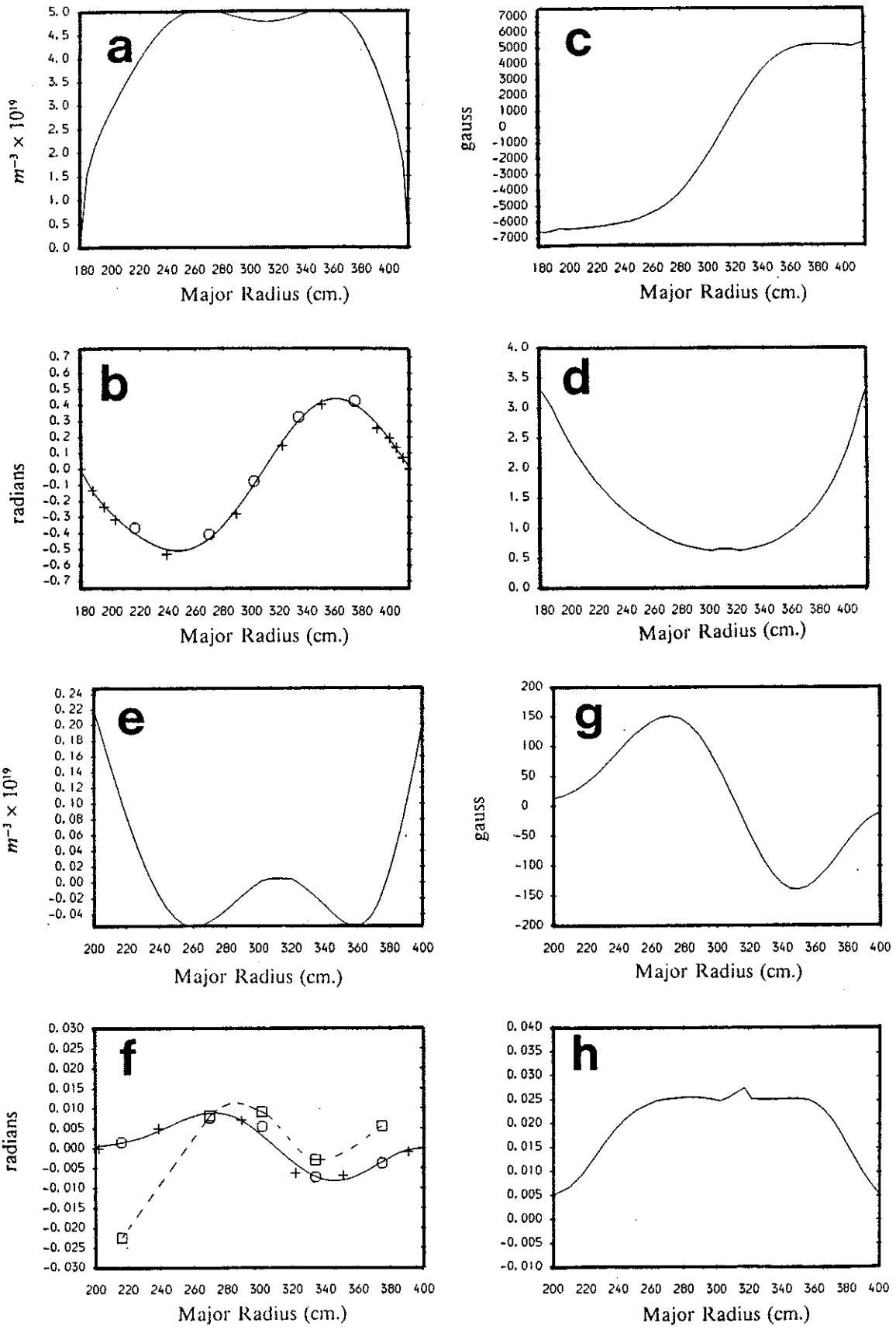

Fig. 3--(a) Electron density profile. (b) Faraday rotation angles. (open circles--data, crosses--virtual data points). (c) Poloidal magnetic field distribution. (d) Safety factor profile. (e) Electron density perturbation. (f) Squares--total perturbed angles, open circles--reduced perturbed angles, crosses--virtual angles. (g) Poloidal field perturbation. (h) Safety factor perturbation.

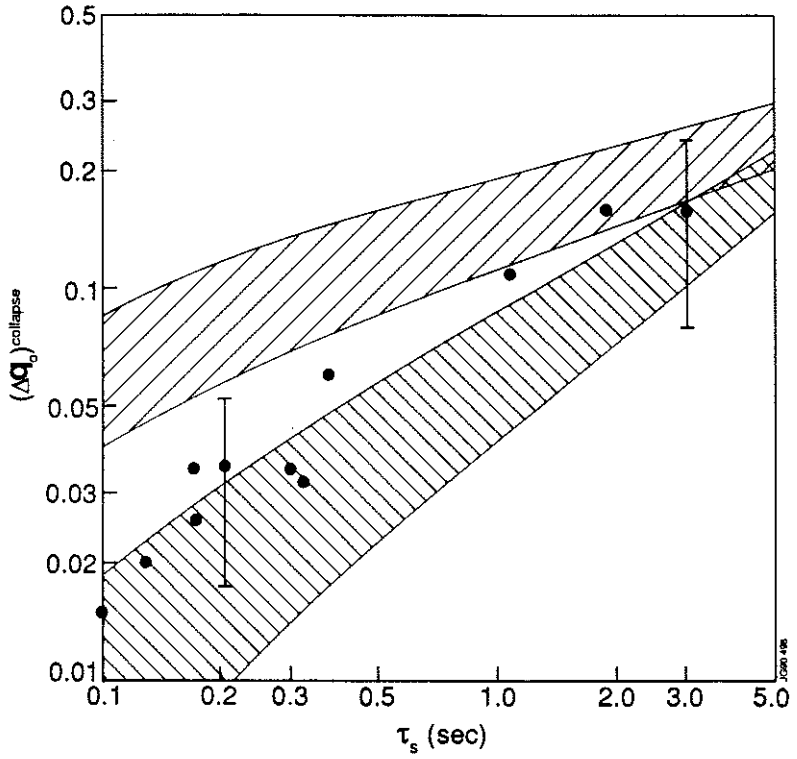

Fig. 4--Change in q_o versus preceding sawtooth period. Circles--data, upper band--field diffusion calculation assuming complete reconnection, lower band--field diffusion calculations assuming $q_o = 0.75$ following the sawtooth collapse.

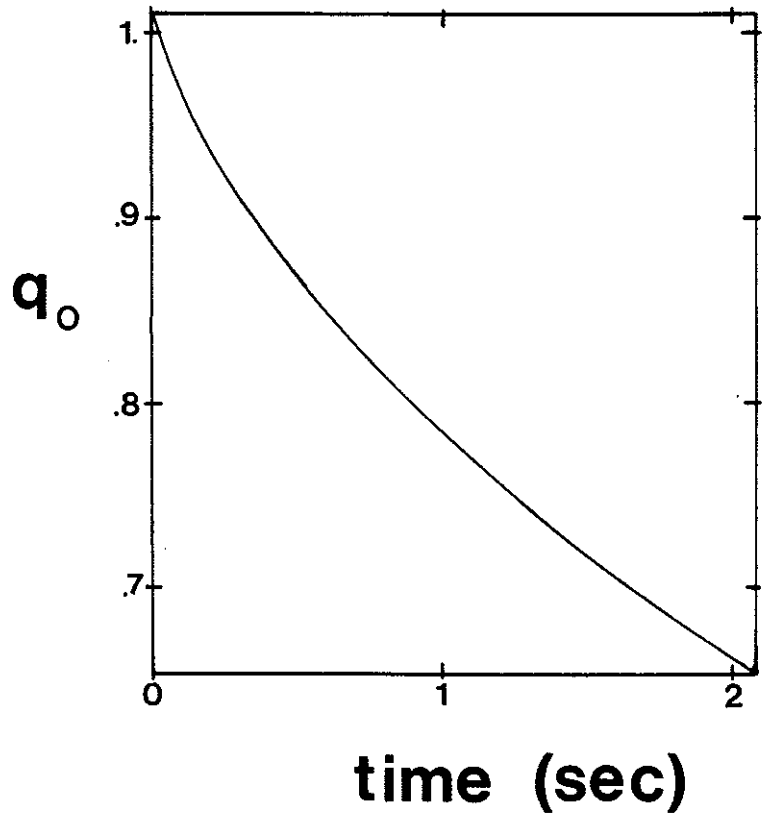

Fig. 5--Evolution of q_o in the absence of sawteeth in a discharge with $I_p = 3MA$, $B_T = 3.4T$, $T_{eo} = 4KeV$, $Z_{eff} = 1.3$, under the assumption of neo-classical resistivity. Note that $\frac{dq_o}{dt}$ decreases as q_o decreases.

APPENDIX 1.

THE JET TEAM

JET Joint Undertaking, Abingdon, Oxon, OX14 3EA, U.K.

J.M.Adams[1], F.Alladio[4], H.Altmann, R.J.Anderson, G.Appruzzese, W.Bailey, B.Balet, D.V.Bartlett, L.R.Baylor[24], K.Behringer, A.C.Bell, P.Bertoldi, E.Bertolini, V.Bhatnagar, R.J.Bickerton, A.Boileau[3], T.Bonicelli, S.J.Booth, G.Bosia, M.Botman, D.Boyd[31], H.Brelen, H.Brinkschulte, M.Brusati, T.Budd, M.Bures, T.Businaro[4], H.Buttgereit, D.Cacaut, C.Caldwell-Nichols, D.J.Campbell, P.Card, J.Carwardine, G.Celentano, P.Chabert[27], C.D.Challis, A.Cheetham, J.Christiansen, C.Christodoulopoulos, P.Chuilon, R.Claesen, S.Clement[30], J.P.Coad, P.Colestock[6], S.Conroy[13], M.Cooke, S.Cooper, J.G.Cordey, W.Core, S.Corti, A.E.Costley, G.Cottrell, M.Cox[7], P.Cripwell[13], F.Crisanti[4], D.Cross, H.de Blank[16], J.de Haas[16], L.de Kock, E.Deksnis, G.B.Denne, G.Deschamps, G.Devillars, K.J.Dietz, J.Dobbing, S.E.Dorling, P.G.Doyle, D.F.Düchs, H.Duquenoy, A.Edwards, J.Ehrenberg[14], T.Elevant[12], W.Engelhardt, S.K.Erents[7], L.G.Eriksonn[5], M.Evrard[2], H.Falter, D.Flory, M.Forrest[7], C.Froger, K.Fullard, M.Gadeberg[11], A.Galetsas, R.Galvao[8], A.Gibson, R.D.Gill, A.Gondhalekar, C.Gordon, G.Gorini, C.Gormezano, N.A.Gottardi, C.Gowers, B.J.Green, F.S.Griph, M.Gryzinski[26], R.Haange, G.Hammett[6], W.Han[9], C.J.Hancock, P.J.Harbour, N.C.Hawkes[7], P.Haynes[7], T.Hellsten, J.L.Hemmerich, R.Hemsworth, R.F.Herzog, K.Hirsch[14], J.Hoekzema, W.A.Houlberg[24], J.How, M.Huart, A.Hubbard, T.P.Hughes[32], M.Hugon, M.Huguet, J.Jacquinot, O.N.Jarvis, T.C.Jernigan[24], E.Joffrin, E.M.Jones, L.P.D.F.Jones, T.T.C.Jones, J.Källne, A.Kaye, B.E.Keen, M.Keilhacker, G.J.Kelly, A.Khare[15], S.Knowlton, A.Konstantellos, M.Kovanen[21], P.Kupschus, P.Lallia, J.R.Last, L.Lauro-Taroni, M.Laux[33], K.Lawson[7], E.Lazzaro, M.Lennholm, X.Litaudon, P.Lomas, M.Lorentz-Gottardi[2], C.Lowry, G.Magyar, D.Maisonnier, M.Malacarne, V.Marchese, P.Massmann, L.McCarthy[28], G.McCracken[7], P.Mendonca, P.Meriguet, P.Micozzi[4], S.F.Mills, P.Millward, S.L.Milora[24], A.Moissonnier, P.L.Mondino, D.Moreau[17], P.Morgan, H.Morsi[14], G.Murphy, M.F.Nave, M.Newman, L.Nickesson, P.Nielsen, P.Noll, W.Obert, D.O'Brien, J.O'Rourke, M.G.Pacco-Düchs, M.Pain, S.Papastergiou, D.Pasini[20], M.Paume[27], N.Peacock[7], D.Pearson[13], F.Pegoraro, M.Pick, S.Pitcher[7], J.Plancoulaine, J-P.Poffé, F.Porcelli, R.Prentice, T.Raimondi, J.Ramette[17], J.M.Rax[27], C.Raymond, P-H.Rebut, J.Removille, F.Rimini, D.Robinson[7], A.Rolfe, R.T.Ross, L.Rossi, G.Rupprecht[14], R.Rushton, P.Rutter, H.C.Sack, G.Sadler, N.Salmon[13], H.Salzmann[14], A.Santagiustina, D.Schissel[25], P.H.Schild, M.Schmid, G.Schmidt[6], R.L.Shaw, A.Sibley, R.Simonini, J.Sips[16], P.Smeulders, J.Snipes, S.Sommers, L.Sonnerup, K.Sonnenberg, M.Stamp, P.Stangeby[19], D.Start, C.A.Steed, D.Stork, P.E.Stott, T.E.Stringer, D.Stubberfield, T.Sugie[18], D.Summers, H.Summers[20], J.Taboda-Duarte[22], J.Tagle[30], H.Tamnen, A.Tanga, A.Taroni, C.Tebaldi[23], A.Tesini, P.R.Thomas, E.Thompson, K.Thomsen[11], P.Trevalion, M.Tschudin, B.Tubbing, K.Uchino[29], E.Usselmann, H.van der Beken, M.von Hellermann, T.Wade, C.Walker, B.A.Wallander, M.Walravens, K.Walter, D.Ward, M.L.Watkins, J.Wesson, D.H.Wheeler, J.Wilks, U.Willen[12], D.Wilson, T.Winkel, C.Woodward, M.Wykes, I.D.Young, L.Zannelli, M.Zarnstorff[6], D.Zasche[14], J.W.Zwart.

PERMANENT ADDRESS

1. UKAEA, Harwell, Oxon. UK.
2. EUR-EB Association, LPP-ERM/KMS, B-1040 Brussels, Belgium.
3. Institute National des Récherches Scientifique, Quebec, Canada.
4. ENEA-CENTRO Di Frascati, I-00044 Frascati, Roma, Italy.
5. Chalmers University of Technology, Göteborg, Sweden.
6. Princeton Plasma Physics Laboratory, New Jersey, USA.
7. UKAEA Culham Laboratory, Abingdon, Oxon. UK.
8. Plasma Physics Laboratory, Space Research Institute, Sao José dos Campos, Brazil.
9. Institute of Mathematics, University of Oxford, UK.
10. CRPP/EPFL, 21 Avenue des Bains, CH-1007 Lausanne, Switzerland.
11. Risø National Laboratory, DK-4000 Roskilde, Denmark.
12. Swedish Energy Research Commission, S-10072 Stockholm, Sweden.
13. Imperial College of Science and Technology, University of London, UK.
14. Max Planck Institut für Plasmaphysik, D-8046 Garching bei München, FRG.
15. Institute for Plasma Research, Gandhinagar Bhat Gujat, India.
16. FOM Instituut voor Plasmafysica, 3430 Be Nieuwegein, The Netherlands.
17. Commissiariat à L'Energie Atomique, F-92260 Fontenay-aux-Roses, France.
18. JAERI, Tokai Research Establishment, Tokai-Mura, Naka-Gun, Japan.
19. Institute for Aerospace Studies, University of Toronto, Downsview, Ontario, Canada.
20. University of Strathclyde, Glasgow, G4 ONG, U.K.
21. Nuclear Engineering Laboratory, Lapeenranta University, Finland.
22. JNICT, Lisboa, Portugal.
23. Department of Mathematics, Univeristy of Bologna, Italy.
24. Oak Ridge National Laboratory, Oak Ridge, Tenn., USA.
25. G.A. Technologies, San Diego, California, USA.
26. Institute for Nuclear Studies, Swierk, Poland.
27. Commissiariat à l'Energie Atomique, Cadarache, France.
28. School of Physical Sciences, Flinders University of South Australia, South Australia SO42.
29. Kyushi University, Kasagu Fukuoka, Japan.
30. Centro de Investigaciones Energeticas Medioambientales y Techalogicas, Spain.
31. University of Maryland, College Park, Maryland, USA.
32. University of Essex, Colchester, UK.
33. Akademie de Wissenschaften, Berlin, DDR.

CR 88.49.1A